On-surface synthesis of unsaturated hydrocarbon chains through C-S activation

Luca Giovanelli, Rémy Pawlak, Fatima Hussein, Oliver Maclean, Federico Rosei, Wentao Song, Corentin Pigot, Frédéric Dumur, Didier Gigmes, Younal Ksari, et al.

On-surface synthesis of unsaturated hydrocarbon chains through C-S activation

Luca Giovanelli [a,*], Rémy Pawlak [b], Fatima Hussein [a], Oliver Maclean [c,d], Federico Rosei [d], Wentao Song [a], Corentin Pigot [e], Frédéric Dumur [e], Didier Gigmes [e], Younal Ksari [a], Federica Bondino[f], Elena Magnano[f,g], Ernst Meyer [b], Sylvain Clair [a,*]

[a] Aix-Marseille Univ, CNRS, IM2NP, Marseille, France.

[b] University of Basel, Department of Physics, Basel CH4056, Switzerland.

[c] Key Laboratory of Functional Materials Physics and Chemistry of the Ministry of Education, Jilin Normal University, Changchun 130103, P. R. China.

[d] Institut National de la Recherche Scientifique, Varennes, Québec J3X 1S2, Canada.

[e] Aix-Marseille Univ, CNRS, ICR, Marseille, France.

[f] IOM-CNR Laboratorio TASC, AREA Science Park, Basovizza, 34149 Trieste, Italy.

[g] Department of Physics, University of Johannesburg, PO Box 524, Auckland Park 2006, South Africa.

* Corresponding authors: luca.giovanelli@im2np.fr ; sylvain.clair@cnrs.fr

Abstract

We use an on-surface synthesis approach to drive the homocoupling reaction of a simple dithiophenyl-functionalized precursor on Cu(111). The C-S activation reaction is initiated at low annealing temperature and yields unsaturated hydrocarbon chains interconnected in a fully conjugated reticulated network. High-resolution atomic force microscopy imaging reveals the opening of the thiophenyl rings and the presence of *trans*- and *cis*-oligoacetylene chains as well as pentalene units. The chemical transformations were studied by C 1s and S 2p core level photoemission spectroscopy and supported by theoretical calculations. At higher annealing temperature, additional cyclization reactions take place, leading to the formation of small graphene flakes.

Keywords: thiophene, homocoupling, polyacetylene, radical coupling reaction, scanning probe microscopy, core-level photoemission spectroscopy

Introduction

A variety of chemical reactions have been explored in on-surface synthesis to create organic compounds by taking advantage of a solid surface acting as a confining template.[1-7] Inspired by the Ullmann reaction, the C-C coupling between halogenated precursors was demonstrated[1] and now represents the most widely used approach. A few other mechanisms have also proven successful, most remarkably the direct C-H activation that is greatly facilitated by the supporting metal surface.[8-11] While alternate reaction pathways have been scarcely proposed,[12-18] it is of prime importance to investigate reaction mechanisms for on-surface synthesis to gain better control and predictability over the reaction products and to position this emerging field as an efficient and versatile chemical synthesis approach.

In traditional solvent-based chemistry the transition metal-mediated activation of C-S bonds has been extensively investigated and sulfur-based organic synthesis is emerging as an alternative to halogen-based synthesis.[19-22] Thiophenyl groups represent an attractive way of introducing sulfur in organic precursors. Thiophene derivatives could be successfully implemented in 3D covalent organic frameworks (COFs) for efficient gap tuning.[23,24] On surfaces, a few covalent networks containing thiophene units have been obtained from Ullmann coupling on Ag(111)[25-27] or Cu(110).[28] Pure polythiophene chains were reported on Au(111) from dibrominated oligothiophenes[29-32] While quaterthiophene and heptathiophene molecules are stable at room temperature on Cu(111),[33] in most cases, a degradation of thiophene derivatives is observed upon thermal activation on reactive surfaces[34] like Cu(111)[25,27,35] or Ni(111).[36,37] Thiophene degradation can be also obtained upon application of an electric field by the STM tip[38] or by applying atomic hydrogen.[39] Successful C-S bond activation has been shown to initiate intra- or inter-molecular reaction on a surface.[37] In this latter work the thiophene units were fused with adjacent benzene rings, which probably limited the reactivity of the as-released radicals and the possibility to extend the polymerization reaction.

We designed the precursor 1,4-di(thiophen-2-yl)benzene (DTB, Fig. 1a)[40,41] as a model system to demonstrate on-surface C-S bond activation as an efficient mechanism to perform C-C coupling at moderate annealing temperature. The thiophene unit in DTB is linked to the core benzene ring through a single C-C bond, a configuration that enables good flexibility compared to a fused thiophene ring.[37] Electropolymerization of this molecule[42,43] and of similar threefold precursors[44-47] has been reported to create materials with good conductivity or electrochromic properties. The polymeric system obtained in this work is fully conjugated and composed mainly of oligoacetylene segments separated by benzene rings. Low-temperature atomic force microscopy (AFM) imaging using CO-terminated tips combined with photoemission spectroscopy and density functional theory (DFT) reveals the structure of the extended polymeric chains, with a mixture of *cis*- and *trans*- polyene as well as pentalene, which are

globally aligned along the substrate high-symmetry directions. Our work thus positions C-S bond activation as an effective strategy in the on-surface synthesis approach, delivering compounds with high potential in molecular electronics applications under mild conditions.

Results and discussion

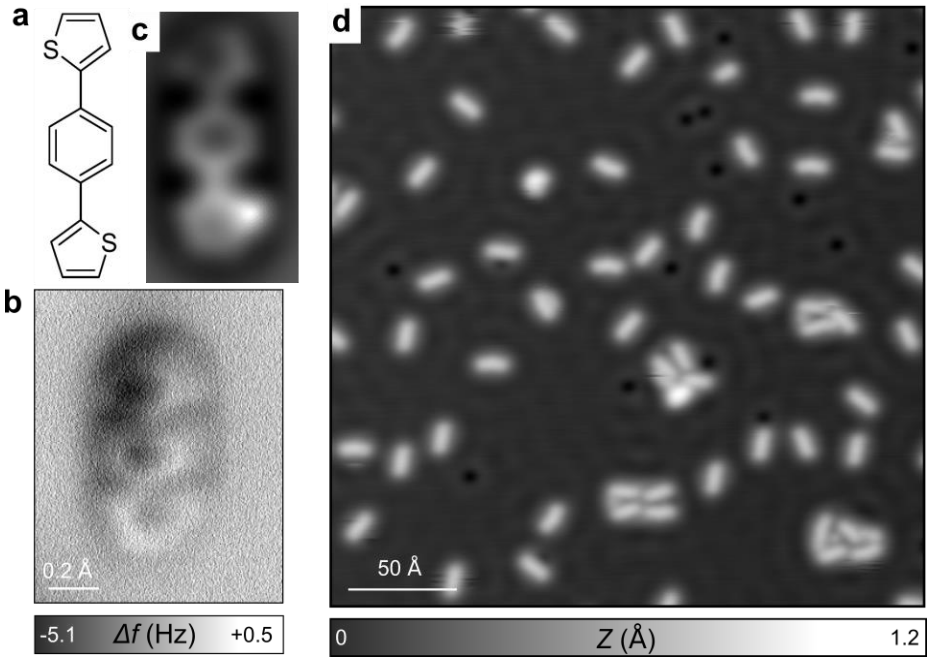

Fig.1.(a) 1,4-di(thiophen-2-yl)benzene (DTB) precursor. (b) High-resolution AFM image of a single DTB obtained with a CO-functionalized tip and (c) corresponding image simulation (DFT). (d) STM image of isolated DTB molecules on Cu(111) acquired at 4.8 K.

DTB molecules were deposited on a Cu(111) surface kept at room temperature in a submonolayer regime. At room temperature the molecules are highly mobile and form a 2D gas phase. Upon cooling the substrate down to 4.8 K, the molecules become immobilized enabling the acquisition of stable scanning tunneling microscopy (STM) images (Fig. 1d). DTB molecules exhibit very weak intermolecular interaction since no large self-assembly can be observed. Figure 1b shows an AFM image using a CO-terminated tip (see Methods) of an isolated molecule that confirms its chemical structure. The molecules remain intact upon sublimation with the benzene and thiophene rings lying almost flat on the surface.[33,48-50] The thiophene rings are slightly tilted and appear elongated by AFM and terminated by a bright protrusion corresponding to the sulfur atom, as confirmed by the simulated AFM image using DFT coordinates of the relaxed DTB structure on Cu(111) (Fig. 1c and SI Fig. S1). Several conformers coexist

on the surface which differ according to the *syn*- or *anti*- orientation of the thiophene units with respect to the central phenyl (see SI Fig. S1).

An annealing temperature of 150°C was required to induce the full C-S activation and the opening of all thiophene rings, although partial reaction could already be observed after 80°C annealing (see Fig. S2). STM images acquired at room temperature (Figs. 2a,b) show the formation of a polymeric network consisting of straight chains up to ~20 nm long and with a tendency to align with the $[1\bar{2}1]$ substrate directions. The chains are randomly interconnected, forming an extended 2D reticulated network. High-resolution AFM images confirmed that the chains consist of the original benzene rings of DTB interconnected by different configurations of oligoacetylene chains (Figs. 2c,d). The chains and benzene rings are resolved with a homogeneous contrast, indicating a perfectly flat adsorption configuration and suggesting that the sulfur atoms were fully removed from the polymer. The contrast of the carbon chains resembles the *trans*- or *cis*-polyacetylene chains that were obtained on Cu(110)[51] and has the periodicity (2.4 Å and 4.4 Å for the *trans*- and the *cis*-chains, respectively). DFT calculations further indicate that the most favorable orientation for the *trans*-chains is along the $[1\bar{1}0]$-direction (see SI Fig. S3a). The *trans*-polyacetylene chains are in principle energetically more favorable than the *cis*-chains,[51] but here the different stereoisomers appear to be locally stochastically distributed, which results in a main orientation of the polymeric chains along the average $[1\bar{2}1]$-directions (Fig. 2).

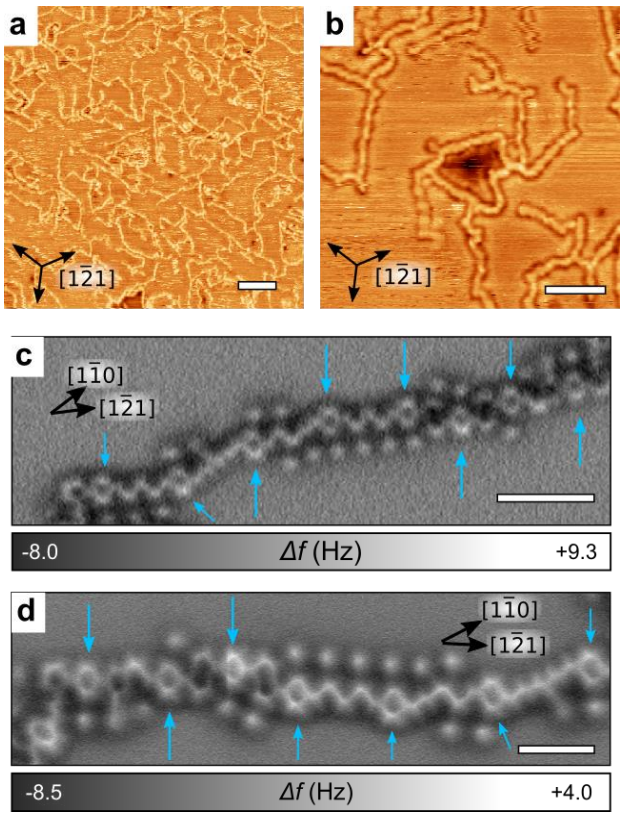

Figure 2. a,b) RT-STM images revealing the on-surface reaction of DTB on Cu(111) after annealing at 150 °C (a) or 200 °C (b). (c,d) High-resolution AFM images of the polymeric chains obtained after annealing at 130°C showing the preserved benzene rings (blue arrows) regularly distributed and linked by linear carbon chains. Scale bars: (a) 10 nm, (b) 4 nm, (c, d) 1 nm.

Figure 3 shows the different reaction products that are formed locally, starting from the desulfurization of the thiophene units. In principle, the thiophene ring opening reaction creates bi-radical species, which couple predominantly at one radical site. The resulting polymeric radical chains are subsequently hydrogenated to produce unsaturated closed shell hydrocarbons (see below).

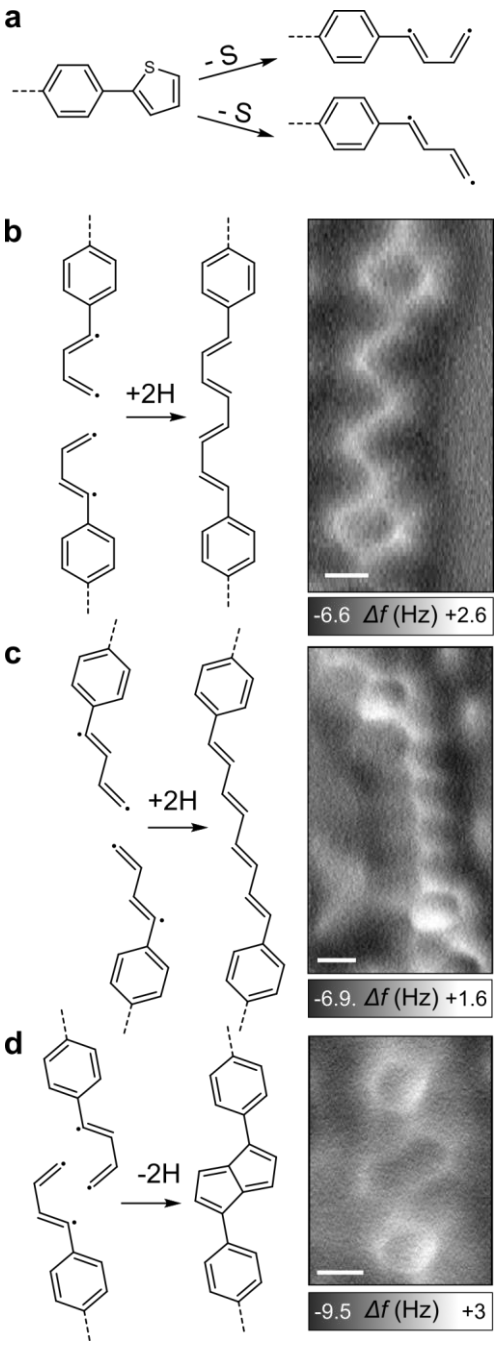

Figure 3. Schematic drawings of the different coupling schemes along with representative high-resolution AFM images. (a) Dissociation of the thiophene rings. Formation of (b) *cis*-oligoacetylene chains, (c) *trans*-oligoacetylene chains and (d) pentalene. Scale bars: 0.2 Å.

Along with *cis*- and *trans*-oligoacetylene chains, pentalene units (Fig. 3d) are also formed occasionally, with an occurrence lower than 20%. The darker contrast measured on these cyclic structures was well reproduced by DFT calculations (SI Fig. S3b). Besides the bifunctional coupling mechanism that creates linear chains, threefold crossing connections are also found. These are responsible for the reticulation of the polymeric network as observed at larger scales (Figs. 2a,b). A high-resolution image of threefold

connections is reproduced in Fig. 4 along with suggestions of their chemical structure. These connections are obtained by coupling of the terminal carbon to the carbon radical closest to the benzene ring. Similar to the formation of pentalene, the creation of these threefold connections allows for a more advanced coupling reaction of the biradical species.

The hydrogenation of radical products is a common process in on-surface synthesis for which the H supply may have different origins. The C-C coupling reaction leading to the formation of pentalene (Fig. 3d) or chain interconnections (Fig. 4) spontaneously releases hydrogen atoms that recombine with the carbon radicals,[52-54] although probably in understoichiometric ratio. The residual hydrogen gas from the vacuum chamber could represent an additional hydrogen source, as it was similarly suggested for various other systems.[55-60] The presence of a carbon radical would lead to strong distortions inside the chains and to a substantial chemical shift[61] of the C 1s core level (see SI Fig. S4) that are not compatible with the perfectly flat contrast of the structures observed in AFM images and XPS data. Also, we never observed products in which the C-S bonds are replaced by C-H bonds without C-C coupling, thus suggesting that the hydrogenation takes place as the last reaction step. Interestingly, no C-Cu bond was identified by XPS at this stage (see corresponding text below). While the complexation of radical species with adatoms is usually observed as an intermediate step in Ullmann-like coupling reactions,[25,61-64] in the present case the C-C coupling followed by hydrogenation takes place without any observable organometallic intermediate.

In addition to the carbon chains, small isolated dots (see Figs. 2c,d) that we can assign as sulfur byproducts are observed in the vicinity of the polymeric chains. They are mostly aligned along the $[1\bar{2}1]$-directions and regularly positioned with an interspacing of 4.3±0.1 Å thus compatible with an epitaxial relationship along this direction (for Cu(111), $a\sqrt{3}$ = 4.4 Å).

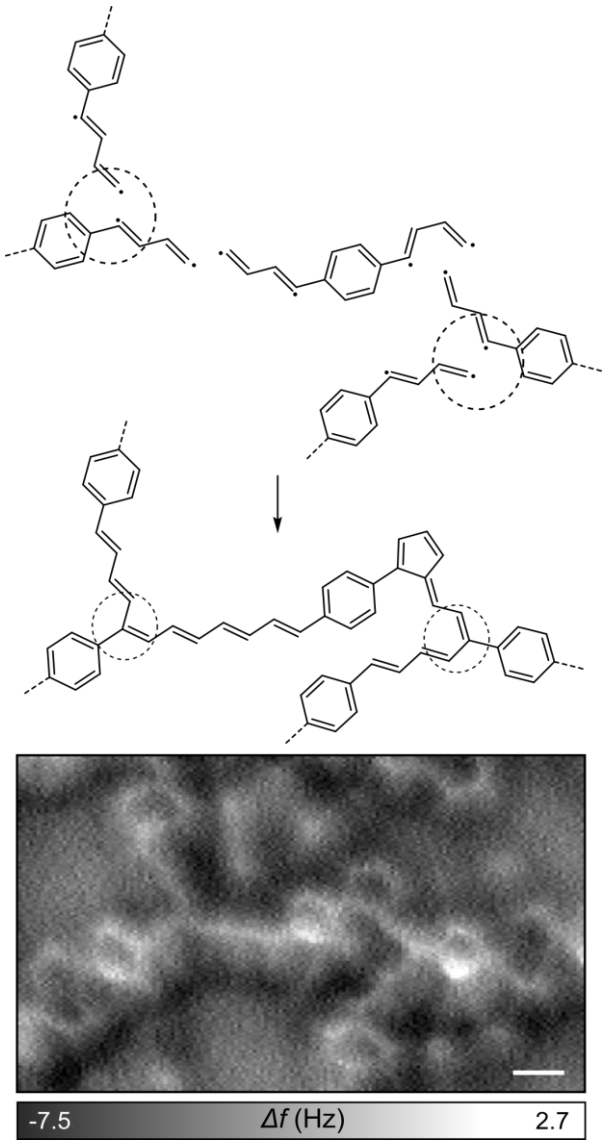

Figure 4. Schematic drawing of the suggested coupling schemes leading to the threefold crossings (dashed circles) along with the corresponding high-resolution AFM image. Scale bar: 2.5 Å.

To gain further insight into the chemistry at play in this system, we acquired temperature-dependent XPS spectra. The S 2p spectrum (Fig. 5a) shows the evolution of the chemical state of S atoms during the polymerization process. The spectrum of a thick layer is used as fingerprint of the pristine molecule. It displays a strong component at a binding energy (BE) of 164.4 eV, in line with other thiophene derivatives on the same surface.[25,35] Least-square fitting gives a full width at half maximum (FWHM) of 0.72 eV, essentially due to intermolecular π-stacking interactions. Two minor components are added to improve the fit which are likely due to different final state screening of surface (high BE) and interface (low BE) molecules.

When a submonolayer is deposited at room temperature, the DTB-derived peak is narrower (FWHM=0.55 eV), close to what is observed in the gas phase for other thiophene derivatives.[65] This is consistent with the 2D gas-phase observed by RT-STM and the consequent reduced intermolecular interaction. The observed shift to lower BE (by -0.24 eV) is characteristic of a reduced film thickness due to the enhanced screening from the metal substrate. An additional minor component at higher BE may be ascribed to a certain preferred adsorption site. At about 3 eV lower BE (between 160.5 and 162.5 eV) a new spectroscopic feature appears revealing atoms having left the molecule upon thiophene ring opening.[25,35] A possible fragmentation of the thiophene into thiolates (e.g. CHS) adsorbed on Cu(111) should give a BE of the $2p_{3/2}$ component around 162.0-162.5 eV,[66-68] which is clearly not observed here. The positions and the line shape rather reveal the presence of atomic S coordinated with Cu.[67,69,70]

When the temperature is increased to 150 °C, i.e. after polymerization, the spectral weight of DTB transfers almost completely into the low BE feature which now distinctively shows three atomic-S derived components at 161.6, 161.2 and 160.7 eV (see also Fig. S5). The first two components were previously reported for sub-ML coverage of S/Cu(111)[69] and can be related to the formation of various S-Cu coordination structures in the vicinity of step edges. In fact, when adsorbed on Cu(111), the high affinity of S to Cu produces mass transport and step edge reconstruction leading to the formation of complex fourfold coordination sites.[71-73] The step edge regions shown in SI Fig. S6 are clearly active sites for molecular adsorption. On the other hand, the lowest BE component at 160.7 eV was not observed in previous studies on atomic sulfur, thiols or thiolates adsorption on Cu(111).[25,35,66,67,69,70] We assign this component to the presence of lower-coordination S, i.e. terrace-supported, threefold-coordinated S. This feature can be traced back to the small protrusions observed beside the polymer chains in the AFM images (see Fig. 2c,d). Such protrusions are smaller than the usual S-Cu complexes[71,72] and are likely to be isolated S atoms restricted from diffusing by the interaction with the just-formed nearby polymers.

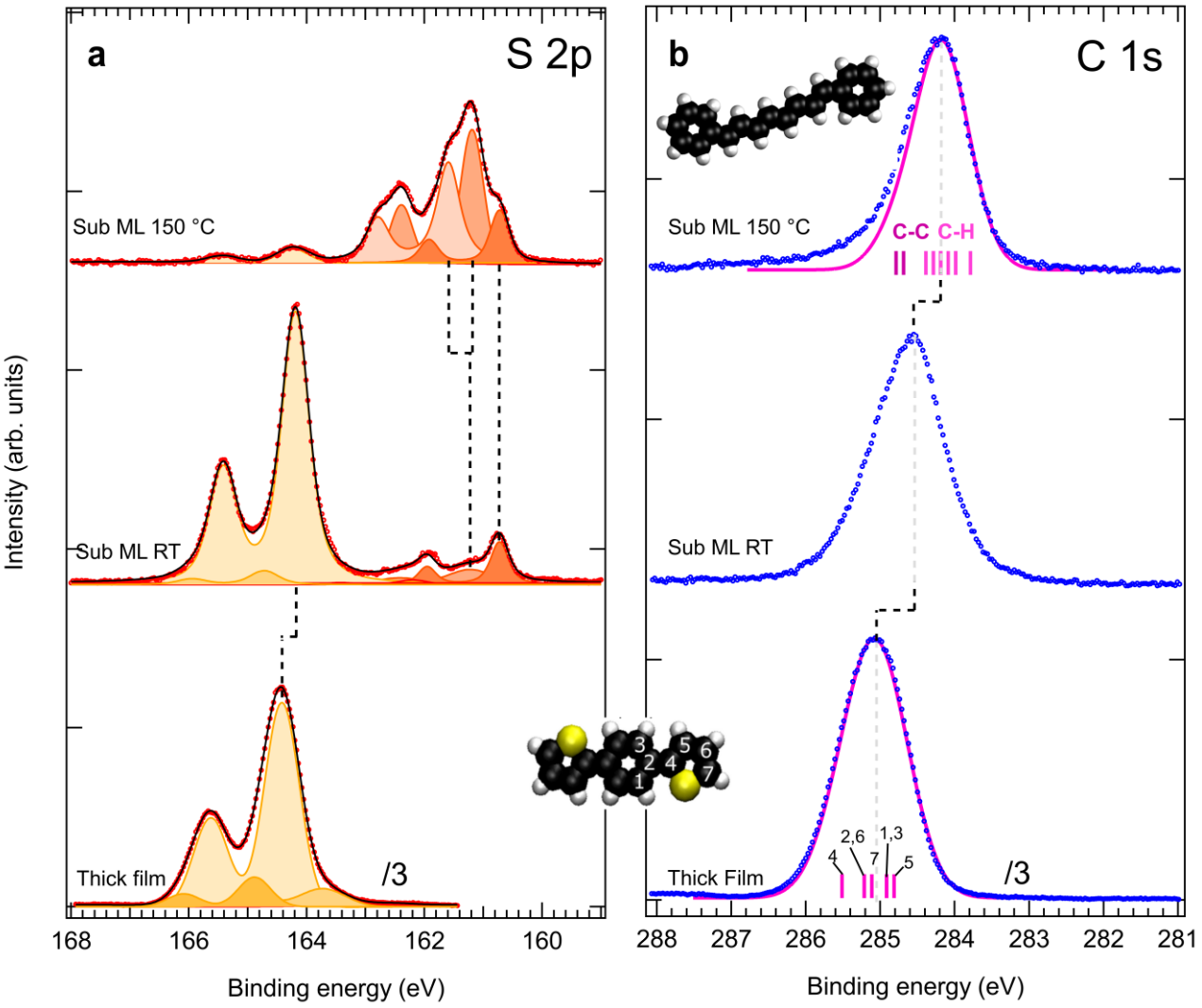

Figure 5. XPS data for DTB/Cu(111). Bottom spectra: a thick film deposited at RT. Upper spectra: sub-ML coverage deposited at RT and annealed at increasing temperatures. (a) S 2p core level (hν = 260 eV). The vertical dashed lines are intended to follow the evolution of the different components (peak fitting) as explained in the text. (b) C 1s core level (hν = 382 eV). Markers: experimental data. Magenta full lines: DFT simulated core levels. For the DTB (thick film) the calculated core levels are numbered according to the inset molecular model. For the polyene chain (sub ML 150°C) the C-C and C-H eigenstates are colored differently.

The C 1s spectrum (Fig. 5b) reflects the presence of C atoms in different oxidation states within the DTB molecule and in the polymeric chains, as well as their interaction with the substrate. When possible, the C 1s spectrum was modeled by DFT calculations. As for the S 2p spectrum, the C 1s of the thick film is representative of the different C atoms in the pristine DTB molecule. The modeling using a DFT-

calculated set of Gaussian components (FWHM of 0.9 eV) represents a good fit for the measured spectrum. The small asymmetry observed at high BE can be attributed to the S-bonded C atom (labeled 4 in inset Fig. 5).

Differently to what is found for S 2p, when a submonolayer of DTB is deposited a visible broadening is observed for C 1s. Additionally, a larger shift of -0.48 eV towards lower BE is observed. This suggests that the molecule-substrate interaction occurs through C atoms (as compared with S atoms) that are found in a number of inequivalent sites with well-screened final states. Part of the broadening at the low-BE side can also be ascribed to the presence of a small fraction of molecules having started to react and lost their S atoms, as revealed by the corresponding S 2p spectrum.

Annealing the sub-ML from RT to 150 °C induces a progressive shift to low BE concurrent with the thiophene ring opening and S release (see SI Fig. S5). At the same time the spectrum narrows, testifying to a more homogeneous sample with well-defined atomic sites within the polymer chains. Its BE and line shape are very similar to those of other 2D polymer-derived spectra.[51,61,74-77] A simple modeling was performed by considering octatetraene chains terminated by two phenyl units adsorbed on the surface (SI Fig. S3a). This model reproduces the overall line shape with a pronounced asymmetry to high BE due to the presence of minority C's having three C-C bonds (the phenyl C's linking the oligoacetylene chains). In the simulated spectra, the inclusion of the Cu(111) surface does not affect the line shape (see Fig. S7). Compared to the simulated model, the real system includes more complex conformations (pentalene structure and threefold connection branches) with a larger C-C to C-H ratio that could be at the origin of the discrepancy in the high BE region. The C-C to C-H BE difference was previously detected in other on-surface polymerization studies involving aromatic compounds,[61,74,76-78] although sometimes with opposite shifts.[75,79,80]

The XPS data shows that the loss of carbon atoms upon annealing is limited to ~3%, in similar proportion as the loss of S (~2%), so we can conclude that most of the carbon and sulfur remain on the surface. The yield of the C-S activated reaction is thus very high and takes place in the range 50 to 120°C (Fig. S5).

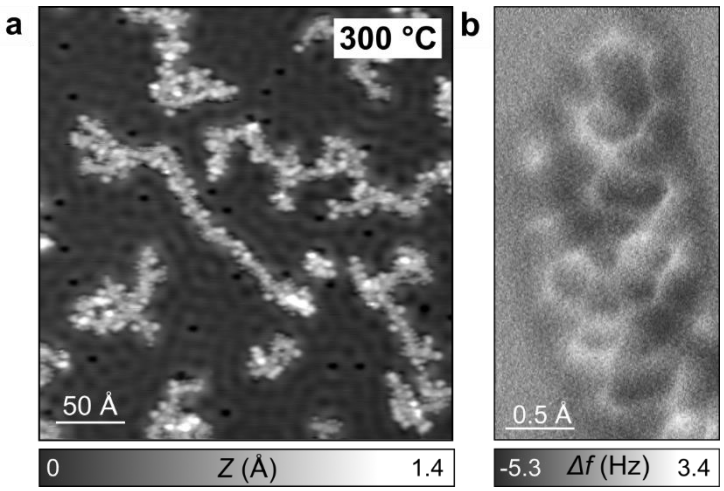

Figure 6. STM (a) and AFM images (b) of DTB/Cu(111) after annealing at 300°C.

Figure 6 shows representative STM and AFM images of the system obtained after annealing at 300°C. We could not observe a transition to the more favorable *trans*-chain configuration,[51] probably due to the strongly reduced mobility in this reticulated network. Similar to the case of polyacetylene chains,[51] cyclization reactions take place and lead to the formation of narrow polyaromatic ribbons. Upon further annealing to 500°C the graphitization reaction is advanced further and small graphene flakes are formed on the surface (see SI Figs. S8, S9). Similar amorphous phases obtained from massive dehydrogenative coupling have been observed for various systems after high temperature annealing of covalent networks on noble metal surfaces.[63,81-86] Indeed graphene formation can take place on a copper surface at sufficiently high temperature from virtually any carbon source.[87,88]

Conclusions and perspectives

We presented the formation of a fully conjugated hydrocarbon polymeric network from simple thiophene-functionalized precursors. The C-S activation at 120°C annealing temperature initiates the formation of carbon radicals that couple to form oligoacetylene chains or pentalene units linking the original benzene rings. Although the coupling reaction is not selective towards *cis*- or *trans*-stereoisomers, the mainly linear chains maintain an overall $[1\bar{2}1]$-orientation along the high symmetry directions of the Cu(111) surface. An alternate reaction mechanism occasionally takes place that leads to the creation of threefold interconnections and the overall formation of a reticulated network. Upon further annealing, additional cyclodehydrogenation reactions occur, leading finally to the formation of small graphene flakes up to a temperature of 500°C.

Our study demonstrates that the strong reactivity of copper toward sulfur-containing species can be exploited to steer an on-surface homocoupling reaction and to create extended polyene chains at low

activation temperature. Unfused thiophene precursors offer simpler synthesis and more diverse coupling chemistry than fused precursors,[37] as they form diradical butadiene moieties instead of ethylene monoradicals. For the synthetic approach in general, C-S activation could be complementary to Ullmann-type coupling as it provides access to antiaromatic and nonbenzenoid structures, such as the pentalene minor product we obtained. However, the precise reaction mechanism still needs to be elucidated, in particular with regard to the role of the atomic sulfur, that is known to affect the bonding of hydrocarbons on Cu(111).[89] Compared to Ullmann-like coupling of halogenated molecules,[25,61-64] no organometallic intermediate was detected, which suggests that the desulfurization step is rate-limiting with respect to both the C-C coupling and the hydrogenation reactions. In future work, different strategies[5] may be explored to improve the order and density of the polymeric network. Preliminary experiments on Cu(110) (see Fig. S10) showed that the strong anisotropy of this surface did not noticeably steer the alignment of the chains, but alternate solutions like e.g. the use of vicinal surfaces,[90] co-adsorbed oxygen[91] or hydrogen,[92] or supramolecular templating[93] may still deliver interesting results. Thiophene groups are sometimes used as constitutive groups in on-surface synthesis on various metal surfaces.[25,27-32] In view of our results showing a relatively low activation temperature of the thiophene ring opening reaction, it is certainly necessary to confirm the integrity of these monomers. Conversely, solutions to preserve the integrity of sulfur in on-surface polymerization reactions include providing an out-of-plane structure of the precursors like in diamantanethiol,[94] or following other strategies that have proved successful to maintain specific functions even on reactive surfaces.[95,96]

Methods

Chemical synthesis of 1,4-di(thiophen-2-yl)benzene

Tetrakis(triphenylphosphine)palladium (0) (0.46 g, 0.744 mmol, M = 1155.56 g.mol^{-1}) was added to a mixture of 1,4-dibromobenzene (1.44 g, 6.11 mmol, M = 235.90 g.mol^{-1}), 2-thiopheneboronic acid (1.62 g, 12.66 mmol, M = 127.96 g.mol^{-1}), toluene (54 mL), ethanol 26 mL) and an aqueous potassium carbonate solution (2 M, 6.91 g in 25 mL water, 26 mL) under vigorous stirring. The mixture was stirred at 80 °C for 48 h under a nitrogen atmosphere. After cooling to room temperature, the reaction mixture was poured into water and extracted with ethyl acetate. The organic layer was washed with brine several times, and the solvent was then evaporated. Addition of DCM followed by pentane precipitated a white solid which was filtered off. The residue was purified by column chromatography (SiO2, pentane/DCM: 1/1 and pure DCM) and isolated as a white solid (1.15 g, 78% yield). ^{1}H NMR, see Fig. S11 (250 MHz,

$CDCl_3$) δ 7.63 (s, 4H), 7.32 (dd, *J* = 11.9, 3.9 Hz, 4H), 7.14 – 7.05 (m, 2H); ^{13}C NMR, see Fig. S12 (63 MHz, $CDCl_3$) δ 143.87, 140.28, 133.45, 128.08, 126.27, 124.88, 123.07, 77.50, 76.99, 76.49; HRMS (ESI MS) m/z: theor: 242.0224 found: 242.0224 (M^+ detected).

Scanning Probe Microscopy

The Cu(111) single crystal was cleaned by repeated cycles of Ar sputtering and annealing. The DTB molecules were deposited from a Knudsen cell maintained at a temperature of 60 to 70°C. The experiments were performed in two different setups. Room-temperature STM was performed with an Omicron VT-STM (typical tunneling parameters 300 pA, -0.5 ~ -1.5V). Low-temperature STM/AFM images were acquired at T = 4.8 K in ultrahigh vacuum ($p \approx 1\times10^{-10}$ mbar) using an Omicron microscope operated with a Nanonis RC5 electronic controller. The force sensor is a commercially available tuning fork sensor based on a qPlus design operated in the frequency-modulation mode (resonance frequency $f_0 \approx 25$ kHz, spring constant $k \approx 1800$ N.m^{-1} , quality factor Q = 14000 and oscillation amplitude A ≈ 0.5 Å). STM images were acquired in constant-current mode with the voltage applied to the tip. AFM measurements were acquired in constant-height mode at V = 0 V. The tip mounted to the qPlus sensor consists in a 25 µm-thick PtIr wire sharpened *ex situ* using a focused ion beam. A clean and sharp Cu tip was then prepared at low temperature by repeated indentations into the substrate. A functionalized tip was created by picking up a single CO molecule from the surface.[97] The images were partly treated with the free software WSxM[98] and Gwyddion.[99]

Photoemission Spectroscopy

XPS was performed *in-situ* with synchrotron radiation at the IOM-CNR BACH beamline (Elettra, Trieste). DTB was evaporated in UHV on the substrate kept at RT. After molecular deposition, the sample was annealed in the analysis chamber (base pressure $1x10^{-9}$ mbar) through a filament at the back of the sample. XPS was performed with a Scienta 3000 electron energy analyzer, in normal emission and using horizontally polarized light. XPS peak fitting of the Shirley background-subtracted S 2p spectra was performed by using Voigt peaks with fixed Lorentzian width of 0.3 eV. The spin-orbit splitting was fixed to the usual 1.2 eV value[65] while the branching ratio was adjusted around the multiplicity value (2:1).

Theoretical modeling

Theoretical calculations were performed with the Vienna *Ab initio* Simulation Package (VASP)[100,101] using the Perdew-Burke-Ernzerhof[102] generalized-gradient approximation (PBE-GGA) for the

exchange-correlation potential, the projector augmented wave (PAW) method,[103,104] and a plane-wave cutoff of 450 eV. The zero-damping DFT-D3 method of Grimme[105] was used for the van der Waals (vdW) correction of the potential energy, and calculations were performed at the gamma *k*-point. Geometry optimizations for the AFM simulations were performed with an (8×8) orthogonal Cu(111) slab constructed using a lattice constant of 0.363 nm and a 1.8 nm vacuum layer, with four atomic layers and the positions of atoms in the bottom two layers fixed (supercell dimensions: 2.05620 nm × 17.8073 nm × 24.2958 nm). Calculations for DTB on Cu(111) used a smaller (6×6) orthogonal slab with the same lattice constant, five atomic layers (bottom two fixed), and a 1.6 nm vacuum layer. The geometries were optimized until the force on each atom was below 0.02 eV/Å. Images of the calculated structures were generated using the VMD software.[106] The AFM image simulation was performed using the Probe Particle model[107,108] for a CO-terminated tip with a charge of 0.05 e, lateral bending stiffness of 0.5 N/m and a particle-tip bond stiffness of 20.0 N/m. The simulated XPS spectra are the result of the convolution of several Gaussians centered at the calculated core level positions (vertical ticks). A negative global shift was applied to the calculated energies to match the maxima of the experimental spectra.

Acknowledgments

G. Galeotti and F. De Marchi are gratefully acknowledged for fruitful discussions, I. Piš and K. Mouhat for technical support. The project leading to this publication received funding from the Excellence Initiative of Aix-Marseille University - A*Midex, a French “Investissements d’Avenir” programme, from Agence Nationale de la Recherche (ANR Grant N° ANR-17-CE08-0010 “DUALITY”). R. P. and E. M. thank financial support from the Swiss National Science Foundation (SNF), the Swiss Nanoscience Institute (SNI) and the European Research Council (ERC) under the European Union’s Horizon 2020 research and innovation programme (ULTRADISS Grant Agreement No. 834402). O.M. acknowledges financial support in the form of a postdoctoral fellowship from Jilin Normal University. F.R. is grateful to the Canada Research Chairs program for partial salary support. The research leading to this result has been supported by the project CALIPSOplus under Grant Agreement 730872 from the EU Framework Programme for Research and Innovation HORIZON 2020.

References

(1) Grill, L.; Dyer, M.; Lafferentz, L.; Persson, M.; Peters, M. V.; Hecht, S. Nano-Architectures by Covalent Assembly of Molecular Building Blocks. *Nat. Nanotechnol.* **2007,** *2*, 687-691.

(2) Clair, S.; Abel, M.; Porte, L. Growth of Boronic Acid Based Two-Dimensional Covalent Networks on a Metal Surface under Ultrahigh Vacuum. *Chem. Commun.* **2014,** *50*, 9627-9635.

(3) Goronzy, D. P.; Ebrahimi, M.; Rosei, F.; Arramel; Fang, Y.; De Feyter, S.; Tait, S. L.; Wang, C.; Beton, P. H.; Wee, A. T. S.; et al. Supramolecular Assemblies on Surfaces: Nanopatterning, Functionality, and Reactivity. *ACS Nano* **2018,** *12*, 7445-7481.

(4) Palmino, F.; Loppacher, C.; Cherioux, F. Photochemistry Highlights on On-Surface Synthesis. *ChemPhysChem* **2019,** *20*, 2271-2280.

(5) Clair, S.; De Oteyza, D. G. Controlling a Chemical Coupling Reaction on a Surface: Tools and Strategies for On-Surface Synthesis. *Chem. Rev.* **2019,** *119*, 4717-4776.

(6) Cui, D.; Perepichka, D. F.; MacLeod, J. M.; Rosei, F. Surface-confined single-layer covalent organic frameworks: design, synthesis and application. *Chem. Soc. Rev.* **2020,** *49*, 2020-2038.

(7) Grill, L.; Hecht, S. Covalent on-surface polymerization. *Nat. Chem.* **2020,** *12*, 115-130.

(8) Zhong, D. Y.; Franke, J. H.; Podiyanachari, S. K.; Blomker, T.; Zhang, H. M.; Kehr, G.; Erker, G.; Fuchs, H.; Chi, L. F. Linear Alkane Polymerization on a Gold Surface. *Science* **2011,** *334*, 213-216.

(9) Gao, H. Y.; Wagner, H.; Zhong, D. Y.; Franke, J. H.; Studer, A.; Fuchs, H. Glaser Coupling at Metal Surfaces. *Angew. Chem. Int. Ed.* **2013,** *52*, 4024-4028.

(10) Li, Q.; Yang, B.; Lin, H. P.; Aghdassi, N.; Miao, K. J.; Zhang, J. J.; Zhang, H. M.; Li, Y. Y.; Duhm, S.; Fan, J.; et al. Surface-Controlled Mono/Diselective ortho C-H Bond Activation. *J. Am. Chem. Soc.* **2016,** *138*, 2809-2814.

(11) Kang, F. M.; Xu, W. On-Surface Synthesis of One-Dimensional Carbon-Based Nanostructures via C-X and C-H Activation Reactions. *ChemPhysChem* **2019,** *20*, 2251-2261.

(12) Gao, H. Y.; Held, P. A.; Amirjalayer, S.; Liu, L. C.; Timmer, A.; Schirmer, B.; Arado, O. D.; Monig, H.; Muck-Lichtenfeld, C.; Neugebauer, J.; et al. Intermolecular On-Surface sigma-Bond Metathesis. *J. Am. Chem. Soc.* **2017,** *139*, 7012-7019.

(13) Liu, L.; Klaasen, H.; Witteler, M. C.; Schulze Lammers, B.; Timmer, A.; Kong, H.; Mönig, H.; Gao, H.-Y.; Neugebauer, J.; Fuchs, H.; et al. Polymerization of silanes through dehydrogenative Si–Si bond formation on metal surfaces. *Nat. Chem.* **2021,** *13*, 350-357.

(14) Kalashnyk, N.; Salomon, E.; Mun, S. H.; Jung, J.; Giovanelli, L.; Angot, T.; Dumur, F.; Gigmes, D.; Clair, S. The Orientation of Silver Surfaces Drives the Reactivity and the Selectivity in Homo‐Coupling Reactions. *ChemPhysChem* **2018,** *19*, 1802-1808.

(15) Galeotti, G.; De Marchi, F.; Hamzehpoor, E.; MacLean, O.; Rao, M. R.; Chen, Y.; Besteiro, L. V.; Dettmann, D.; Ferrari, L.; Frezza, F.; et al. Synthesis of mesoscale ordered two-dimensional pi-conjugated polymers with semiconducting properties. *Nat. Mater.* **2020,** *19*, 874-880.

(16) Wang, S. S.; Li, Z.; Ding, P. C.; Mattioli, C.; Huang, W. J.; Wang, Y.; Gourdon, A.; Sun, Y.; Chen, M. S.; Kantorovich, L.; et al. On-Surface Decarboxylation Coupling Facilitated by Lock-to-Unlock Variation of Molecules upon the Reaction. *Angew. Chem. Int. Ed.* **2021,** *60*, 17435-17439.

(17) Han, D.; Zhu, J. F. Surface-assisted fabrication of low-dimensional carbon-based nanoarchitectures. *J. Phys. Condens. Matter.* **2021,** *33*, 36.

(18) Holec, J.; Cogliati, B.; Lawrence, J.; Berdonces-Layunta, A.; Herrero, P.; Nagata, Y.; Banasiewicz, M.; Kozankiewicz, B.; Corso, M.; Oteyza, D. G.; et al. A Large Starphene Comprising Pentacene Branches. *Angew. Chem. Int. Ed.* **2021,** *60*, 7752-7758.

(19) Wang, L. D.; He, W.; Yu, Z. K. Transition-Metal Mediated Carbon-Sulfur Bond Activation and Transformations. *Chem. Soc. Rev.* **2013,** *42*, 599-621.

(20) Otsuka, S.; Nogi, K.; Yorimitsu, H. C-S Bond Activation. *Top. Curr. Chem.* **2018,** *376*, 39.

(21) D'Auria, M. In *Advances in Heterocyclic Chemistry, Vol 104*; Katritzky, A. R., Ed.; Elsevier Academic Press Inc: San Diego, 2011; Vol. 104; p 127-390.

(22) Li, J.; Huang, H. N.; Liang, W. H.; Gao, Q.; Duan, Z. Catalytic C-H and C-S Bond Activation of Thiophenes. *Org. Lett.* **2013,** *15*, 282-285.

(23) Bertrand, G. H. V.; Michaelis, V. K.; Ong, T. C.; Griffin, R. G.; Dinca, M. Thiophene-based covalent organic frameworks. *Proc. Natl. Acad. Sci. U.S.A.* **2013,** *110*, 4923-4928.

(24) Ball, B.; Chakravarty, C.; Mandal, B.; Sarkar, P. Computational Investigation on the Electronic Structure and Functionalities of a Thiophene-Based Covalent Triazine Framework. *Acs Omega* **2019,** *4*, 3556-3564.

(25) Gutzler, R.; Cardenas, L.; Lipton-Duffin, J.; El Garah, M.; Dinca, L. E.; Szakacs, C. E.; Fu, C. Y.; Gallagher, M.; Vondracek, M.; Rybachuk, M.; et al. Ullmann-Type Coupling of Brominated Tetrathienoanthracene on Copper and Silver. *Nanoscale* **2014,** *6*, 2660-2668.

(26) Cardenas, L.; Gutzler, R.; Lipton-Duffin, J.; Fu, C. Y.; Brusso, J. L.; Dinca, L. E.; Vondracak, M.; Fagot-Revurat, Y.; Malterre, D.; Rosei, F.; et al. Synthesis and electronic structure of a two dimensional pi-conjugated polythiophene. *Chem. Sci.* **2013,** *4*, 3263-3268.
(27) Di Bernardo, I.; Hines, P.; Abyazisani, M.; Motta, N.; MacLeod, J.; Lipton-Duffin, J. On-Surface Synthesis of Polyethylenedioxythiophene. *Chem. Commun.* **2018,** *54*, 3723-3726.
(28) Lipton-Duffin, J. A.; Miwa, J. A.; Kondratenko, M.; Cicoira, F.; Sumpter, B. G.; Meunier, V.; Perepichka, D. F.; Rosei, F. Step-by-Step Growth of Epitaxially Aligned Polythiophene by Surface-Confined Reaction. *Proc. Natl. Acad. Sci. U.S.A.* **2010,** *107*, 11200-11204.
(29) Lu, J. C.; Yang, X. T.; Hao, Z. L.; Du, R. J.; Wang, X. Y.; Tan, H. L.; Yan, C. X.; Cai, J. M.; Lin, X.; Du, S. On-Surface Synthesis and Characterization of Polythiophene Chains. *J. Phys. Chem. C* **2020,** *124*, 764-768.
(30) Liu, L. Q.; Miao, X. R.; Shi, T. T.; Liu, X. G.; Yip, H. L.; Deng, W. L.; Cao, Y. Conformation modification of terthiophene during the on-surface synthesis of pure polythiophene. *Nanoscale* **2020,** *12*, 18096-18105.
(31) Reecht, G.; Bulou, H.; Scheurer, F.; Speisser, V.; Carriere, B.; Mathevet, F.; Schull, G. Oligothiophene Nanorings as Electron Resonators for Whispering Gallery Modes. *Phys. Rev. Lett.* **2013,** *110*, 056802.
(32) Liu, L. Q.; Zou, H. Q.; Miao, X. R.; Yip, H. L.; Deng, W. L.; Cao, Y. Stepwise on-surface synthesis of thiophene-based polymeric ribbons by coupling reactions and the carbon-fluorine bond cleavage. *Phys. Chem. Chem. Phys.* **2021**, DOI:10.1039/d1cp04039a 10.1039/d1cp04039a, Advance Article.
(33) Kakudate, T.; Tsukamoto, S.; Kubo, O.; Nakaya, M.; Nakayama, T. Electronic Structures of Quaterthiophene and Septithiophene on Cu(111): Spatial Distribution of Adsorption-Induced States Studied by STM and DFT Calculation. *J. Phys. Chem. C* **2016,** *120*, 6681-6688.
(34) Malone, W.; Kaden, W.; Kara, A. Exploring Thiophene Desulfurization: The Adsorption of Thiophene on Transition Metal Surfaces. *Surf. Sci.* **2019,** *686*, 30-38.
(35) Galeotti, G.; De Marchi, F.; Taerum, T.; Besteiro, L. V.; El Garah, M.; Lipton-Duffin, J.; Ebrahimi, M.; Perepichka, D. F.; Rosei, F. Surface-Mediated Assembly, Polymerization and Degradation of Thiophene-Based Monomers. *Chem. Sci.* **2019,** *10*, 5167-5175.
(36) Dinca, L. E.; Fu, C. Y.; MacLeod, J. M.; Lipton-Duffin, J.; Brusso, J. L.; Szakacs, C. E.; Ma, D. L.; Perepichka, D. F.; Rosei, F. Unprecedented Transformation of Tetrathienoanthracene into Pentacene on Ni(111). *ACS Nano* **2013,** *7*, 1652-1657.
(37) Dinca, L. E.; MacLeod, J. M.; Lipton-Duffin, J.; Fu, C. Y.; Ma, D. L.; Perepichka, D. F.; Rosei, F. Tailoring the Reaction Path in the On-Surface Chemistry of Thienoacenes. *J. Phys. Chem. C* **2015,** *119*, 22432-22438.
(38) Borca, B.; Michnowicz, T.; Petuya, R.; Pristl, M.; Schendel, V.; Pentegov, I.; Kraft, U.; Klauk, H.; Wahl, P.; Gutzler, R.; et al. Electric-Field-Driven Direct Desulfurization. *ACS Nano* **2017,** *11*, 4703-4709.
(39) Zuzak, R.; Jancarik, A.; Gourdon, A.; Szymonski, M.; Godlewski, S. On-Surface Synthesis with Atomic Hydrogen. *ACS Nano* **2020,** *14*, 13316-13323.
(40) Tamao, K.; Kodama, S.; Nakajima, I.; Kumada, M.; Minato, A.; Suzuki, K. Nickel-phosphine complex-catalyzed Grignard coupling - II : Grignard coupling of heterocyclic compounds. *Tetrahedron* **1982,** *38*, 3347-3354.
(41) Yang, M. J.; Zhang, Q. H.; Wu, P.; Ye, H.; Liu, X. Influence of the Introduction of Phenylene Units into the Polymer Backbone on Bandgap of Conjugated Poly(Heteroarylene Methines). *Polymer* **2005,** *46*, 6266-6273.
(42) Danieli, R.; Ostoja, P.; Tiecco, M.; Zamboni, R.; Taliani, C. Poly[1,4-di-(2-Thienyl)Benzene]: a New Conducting Polymer. *J. Chem. Soc., Chem. Commun.* **1986**, 1473-1474.
(43) Xu, L. Y.; Zhao, J. S.; Cui, C. S.; Liu, R. M.; Liu, J. F.; Wang, H. S. Electrosynthesis and Characterization of an Electrochromic Material from Poly(1,4-bis(2-Thienyl)-Benzene) and its Application in Electrochromic Devices. *Electrochim. Acta* **2011,** *56*, 2815-2822.
(44) Idzik, K. R.; Beckert, R.; Golba, S.; Ledwon, P.; Lapkowski, M. Synthesis by Stille Cross-Coupling Procedure and Electrochemical Properties of C3-Symmetric Oligoarylobenzenes. *Tetrahedron Lett.* **2010,** *51*, 2396-2399.
(45) Nakae, T.; Mizobuchi, S.; Yano, M.; Ukai, T.; Sato, H.; Shinmei, T.; Inoue, T.; Irifune, T.; Sakaguchi, H. Benzo[b]trithiophene Polymer Network Prepared by Electrochemical Polymerization with a Combination of Thermal Conversion. *Chem. Lett.* **2012,** *41*, 140-141.
(46) Gu, C.; Huang, N.; Chen, Y. C.; Qin, L. Q.; Xu, H.; Zhang, S. T.; Li, F. H.; Ma, Y. G.; Jiang, D. L. pi-Conjugated Microporous Polymer Films: Designed Synthesis, Conducting Properties, and Photoenergy Conversions. *Angew. Chem. Int. Ed.* **2015,** *54*, 13594-13598.
(47) Ledwon, P.; Turczyn, R.; Idzik, K. R.; Beckert, R.; Frydel, J.; Lapkowski, M.; Domagala, W. Doping Behaviour of Electrochemically Generated Model Bithiophene Meta-Substituted Star Shaped Oligomer. *Mater. Chem. Phys.* **2014,** *147*, 254-260.
(48) Malone, W.; Matos, J.; Kara, A. Adsorption of Thiophene on Transition Metal Surfaces with the Inclusion of van der Waals Effects. *Surf. Sci.* **2018,** *669*, 121-129.
(49) Richardson, N. V.; Campuzano, J. C. The adsorption of thiophene on a Cu(111) surface. *Vacuum* **1981,** *31*, 449-451.
(50) Milligan, P. K.; Murphy, B.; Lennon, D.; Cowie, B. C. C.; Kadodwala, M. A complete structural study of the coverage dependence of the bonding of thiophene on Cu(111). *J. Phys. Chem. B* **2001,** *105*, 140-148.

(51) Wang, S. Y.; Sun, Q.; Groning, O.; Widmer, R.; Pignedoli, C. A.; Cai, L. L.; Yu, X.; Yuan, B. K.; Li, C.; Ju, H. X.; et al. On-surface synthesis and characterization of individual polyacetylene chains. *Nat. Chem.* **2019,** *11*, 924-930.
(52) Wackerlin, C.; Gallardo, A.; Mairena, A.; Baljozovic, M.; Cahlik, A.; Antalik, A.; Brabec, J.; Veis, L.; Nachtigallova, D.; Jelinek, P.; et al. On-Surface Hydrogenation of Buckybowls: From Curved Aromatic Molecules to Planar Non-Kekule Aromatic Hydrocarbons. *ACS Nano* **2020,** *14*, 16735-16742.
(53) Castro-Esteban, J.; Albrecht, F.; Fatayer, S.; Perez, D.; Gross, L.; Pena, D. An on-surface Diels-Alder reaction. *Angew. Chem. Int. Ed.* **2021,** *60*, 26346-26350.
(54) Ma, C. X.; Xiao, Z. C.; Bonnesen, P. V.; Liang, L. B.; Puretzky, A. A.; Huang, J. S.; Kolmer, M.; Sumpter, B. G.; Lu, W. C.; Hong, K. L.; et al. On-surface cyclodehydrogenation reaction pathway determined by selective molecular deuterations. *Chem. Sci.* **2021,** *12*, 15637-15644.
(55) Canas-Ventura, M. E.; Klappenberger, F.; Clair, S.; Pons, S.; Kern, K.; Brune, H.; Strunskus, T.; Woll, C.; Fasel, R.; Barth, J. V. Coexistence of One- and Two-Dimensional Supramolecular Assemblies of Terephthalic Acid on Pd(111) due to Self-Limiting Deprotonation. *J. Chem. Phys.* **2006,** *125*, 184710.
(56) Urgel, J. I.; Di Giovannantonio, M.; Gandus, G.; Chen, Q.; Liu, X. S.; Hayashi, H.; Ruffieux, P.; Decurtins, S.; Narita, A.; Passerone, D.; et al. Overcoming Steric Hindrance in Aryl-Aryl Homocoupling via On-Surface Copolymerization. *ChemPhysChem* **2019,** *20*, 2360-2366.
(57) Sanchez-Grande, A.; Urgel, J. I.; Veis, L.; Edalatmanesh, S.; Santos, J.; Lauwaet, K.; Mutombo, P.; Gallego, J. M.; Brabec, J.; Beran, P.; et al. Unravelling the Open-Shell Character of Peripentacene on Au(111). *J. Phys. Chem. Lett.* **2021,** *12*, 330-336.
(58) Cirera, B.; de la Torre, B.; Moreno, D.; Ondracek, M.; Zboril, R.; Miranda, R.; Jelinek, P.; Ecija, D. On-Surface Synthesis of Gold Porphyrin Derivatives via a Cascade of Chemical Interactions: Planarization, Self-Metalation, and Intermolecular Coupling. *Chem. Mater.* **2019,** *31*, 3248-3256.
(59) Kawai, S.; Takahashi, K.; Ito, S.; Pawlak, R.; Meier, T.; Spijker, P.; Canova, F. F.; Tracey, J.; Nozaki, K.; Foster, A. S.; et al. Competing Annulene and Radialene Structures in a Single Anti-Aromatic Molecule Studied by High-Resolution Atomic Force Microscopy. *ACS Nano* **2017,** *11*, 8122-8130.
(60) Zhang, C.; Kazuma, E.; Kim, Y. Atomic-Scale Visualization of the Stepwise Metal-Mediated Dehalogenative Cycloaddition Reaction Pathways: Competition between Radicals and Organometallic Intermediates. *Angew. Chem. Int. Ed.* **2019,** *58*, 17736-17744.
(61) Simonov, K. A.; Vinogradov, N. A.; Vinogradov, A. S.; Generalov, A. V.; Zagrebina, E. M.; Martensson, N.; Cafolla, A. A.; Carpy, T.; Cunniffe, J. P.; Preobrajenski, A. B. Effect of Substrate Chemistry on the Bottom-Up Fabrication of Graphene Nanoribbons: Combined Core-Level Spectroscopy and STM Study. *J. Phys. Chem. C* **2014,** *118*, 12532-12540.
(62) Sun, Q.; Cai, L. L.; Ma, H. H.; Yuan, C. X.; Xu, W. The Stereoselective Synthesis of Dienes through Dehalogenative Homocoupling of Terminal Alkenyl Bromides on Cu(110). *Chem. Commun.* **2016,** *52*, 6009-6012.
(63) Ferrighi, L.; Pis, I.; Nguyen, T. H.; Cattelan, M.; Nappini, S.; Basagni, A.; Parravicini, M.; Papagni, A.; Sedona, F.; Magnano, E.; et al. Control of the Intermolecular Coupling of Dibromotetracene on Cu(110) by the Sequential Activation of C-Br and C-H Bonds. *Chem. Eur. J.* **2015,** *21*, 5826-5835.
(64) Dong, L.; Wang, S.; Wang, W.; Chen, C.; Lin, T.; Adisoejoso, J.; Lin, N. In *On-Surface Synthesis*; Gourdon, S., Ed.; Springer-Verlag: Berlin, 2016; p 23-42.
(65) Zhang, T.; Brumboiu, I. E.; Grazioli, C.; Guarnaccio, A.; Coreno, M.; de Simone, M.; Santagata, A.; Rensmo, H.; Brena, B.; Lanzilotto, V.; et al. Lone-Pair Delocalization Effects within Electron Donor Molecules: The Case of Triphenylamine and Its Thiophene-Analog. *J. Phys. Chem. C* **2018,** *122*, 17706-17717.
(66) Jia, J. J.; Giglia, A.; Flores, M.; Grizzi, O.; Pasquali, L.; Esaulov, V. A. 1,4-Benzenedimethanethiol Interaction with Au(110), Ag(111), Cu(100), and Cu(111) Surfaces: Self-Assembly and Dissociation Processes. *J. Phys. Chem. C* **2014,** *118*, 26866-26876.
(67) Sirtl, T.; Lischka, M.; Eichhorn, J.; Rastgoo-Lahrood, A.; Strunskus, T.; Heckl, W. M.; Lackinger, M. From Benzenetrithiolate Self-Assembly to Copper Sulfide Adlayers on Cu(111): Temperature-Induced Irreversible and Reversible Phase Transitions. *J. Phys. Chem. C* **2014,** *118*, 3590-3598.
(68) Meng, X. Z.; Kolodzeiski, E.; Huang, X.; Timmer, A.; Lammers, B. S.; Gao, H. Y.; Monig, H.; Liu, L. C.; Xu, W.; Amirjalayer, S.; et al. Tunable Thiolate Coordination Networks on Metal Surfaces. *Chemnanomat* **2020,** *6*, 1479-1484.
(69) Wahlstrom, E.; Ekvall, I.; Olin, H.; Lindgren, S. A.; Wallden, L. Observation of ordered structures for S/Cu(111) at low temperature and coverage. *Phys. Rev. B* **1999,** *60*, 10699-10702.
(70) Jia, J. J.; Bendounan, A.; Chaouchi, K.; Esaulov, V. A. Sulfur Interaction with Cu(100) and Cu(111) Surfaces: A Photoemission Study. *J. Phys. Chem. C* **2014,** *118*, 24583-24590.
(71) Walen, H.; Liu, D. J.; Oh, J.; Lim, H.; Evans, J. W.; Aikens, C. M.; Kim, Y.; Thiel, P. A. Cu_2S_3 complex on Cu(111) as a candidate for mass transport enhancement. *Phys. Rev. B* **2015,** *91*, 045426.
(72) Walen, H.; Liu, D. J.; Oh, J.; Lim, H.; Evans, J. W.; Kim, Y.; Thiel, P. A. Reconstruction of steps on the Cu(111) surface induced by sulfur. *J. Chem. Phys.* **2015,** *142*, 194711.

(73) Liu, D. J.; Spurgeon, P. M.; Lee, J.; Windus, T. L.; Thiel, P. A.; Evans, J. W. Sulfur adsorption on coinage metal(100) surfaces: propensity for metal-sulfur complex formation relative to (111) surfaces. *Phys. Chem. Chem. Phys.* **2019,** *21*, 26483-26491.

(74) Moreno, C.; Panighel, M.; Vilas-Varela, M.; Sauthier, G.; Tenorio, M.; Ceballos, G.; Pena, D.; Mugarza, A. Critical Role of Phenyl Substitution and Catalytic Substrate in the Surface-Assisted Polymerization of Dibromobianthracene Derivatives. *Chem. Mater.* **2019,** *31*, 331-341.

(75) Pis, I.; Ferrighi, L.; Nguyen, T. H.; Nappini, S.; Vaghi, L.; Basagni, A.; Magnano, E.; Papagni, A.; Sedona, F.; Di Valentin, C.; et al. Surface-Confined Polymerization of Halogenated Polyacenes: The Case of Dibromotetracene on Ag(110). *J. Phys. Chem. C* **2016,** *120*, 4909-4918.

(76) Basagni, A.; Sedona, F.; Pignedoli, C. A.; Cattelan, M.; Nicolas, L.; Casarin, M.; Sambi, M. Molecules-Oligomers-Nanowires-Graphene Nanoribbons: A Bottom-Up Stepwise On-Surface Covalent Synthesis Preserving Long-Range Order. *J. Am. Chem. Soc.* **2015,** *137*, 1802-1808.

(77) Panighel, M.; Quiroga, S.; Brandimarte, P.; Moreno, C.; Garcia-Lekue, A.; Vilas-Varela, M.; Rey, D.; Sauthier, G.; Ceballos, G.; Pena, D.; et al. Stabilizing Edge Fluorination in Graphene Nanoribbons. *ACS Nano* **2020,** *14*, 11120-11129.

(78) Cirera, B.; Riss, A.; Mutombo, P.; Urgel, J. I.; Santos, J.; Di Giovannantonio, M.; Widmer, R.; Stolz, S.; Sun, Q.; Bommert, M.; et al. On-surface synthesis of organocopper metallacycles through activation of inner diacetylene moieties. *Chem. Sci.* **2021,** *12*, 12806-12811.

(79) Fan, Q. T.; Yan, L. H.; Tripp, M. W.; Krejci, O.; Dimosthenous, S.; Kachel, S. R.; Chen, M. Y.; Foster, A. S.; Koert, U.; Liljeroth, P.; et al. Biphenylene network: A nonbenzenoid carbon allotrope. *Science* **2021,** *372*, 852-856.

(80) Savu, S. A.; Casu, M. B.; Schundelmeier, S.; Abb, S.; Tonshoff, C.; Bettinger, H. F.; Chasse, T. Nanoscale assembly, morphology and screening effects in nanorods of newly synthesized substituted pentacenes. *RSC Adv.* **2012,** *2*, 5112-5118.

(81) Rabia, A.; Tumino, F.; Milani, A.; Russo, V.; Li Bassi, A.; Bassi, N.; Lucotti, A.; Achilli, S.; Fratesi, G.; Manini, N.; et al. Structural, Electronic, and Vibrational Properties of a Two-Dimensional Graphdiyne-like Carbon Nanonetwork Synthesized on Au(111): Implications for the Engineering of sp-sp(2) Carbon Nanostructures. *Acs Applied Nano Materials* **2020,** *3*, 12178-12187.

(82) Sedona, F.; Fakhrabadi, M. M. S.; Carlotto, S.; Mohebbi, E.; De Boni, F.; Casalini, S.; Casarin, M.; Sambi, M. On-surface synthesis of extended linear graphyne molecular wires by protecting the alkynyl group. *Phys. Chem. Chem. Phys.* **2020,** *22*, 12180-12186.

(83) Lischka, M.; Michelitsch, G. S.; Martsinovich, N.; Eichhorn, J.; Rastgoo-Lahrood, A.; Strunskus, T.; Breuer, R.; Reuter, K.; Schmittel, M.; Lackinger, M. Remote Functionalization in Surface-Assisted Dehalogenation by Conformational Mechanics: Organometallic Self-Assembly of 3,3 ',5,5 '-Tetrabromo-2,2 ',4,4 ',6,6 '-Hexafluorobiphenyl on Ag(111). *Nanoscale* **2018,** *10*, 12035-12044.

(84) Huang, J. M.; Jia, H. X.; Wang, T.; Feng, L.; Du, P. W.; Zhu, J. F. Kinetic Control over Morphology of Nanoporous Graphene on Surface. *ChemPhysChem* **2019,** *20*, 2327-2332.

(85) del Arbol, N. R.; Sanchez-Sanchez, C.; Otero-Irurueta, G.; Martinez, J. I.; de Andres, P. L.; Gomez-Herrero, A. C.; Merino, P.; Piantek, M.; Serrate, D.; Lacovig, P.; et al. On-Surface Driven Formal Michael Addition Produces m-Polyaniline Oligomers on Pt(111). *Angew. Chem. Int. Ed.* **2020,** *59*, 23220-23227.

(86) Smerieri, M.; Pis, I.; Ferrighi, L.; Nappini, S.; Lusuan, A.; Vattuone, L.; Vaghi, L.; Papagni, A.; Magnano, E.; Di Valentin, C.; et al. Synthesis of Corrugated C-Based Nanostructures by Br-Corannulene Oligomerization. *Phys. Chem. Chem. Phys.* **2018,** *20*, 26161-26172.

(87) Ruan, G. D.; Sun, Z. Z.; Peng, Z. W.; Tour, J. M. Growth of Graphene from Food, Insects, and Waste. *ACS Nano* **2011,** *5*, 7601-7607.

(88) Zhang, J. C.; Lin, L.; Jia, K. C.; Sun, L. Z.; Peng, H. L.; Liu, Z. F. Controlled Growth of Single-Crystal Graphene Films. *Adv. Mater.* **2020,** *32*, 1903266.

(89) Rousseau, G. B. D.; Bovet, N.; Kadodwala, M. Sulfur the archetypal catalyst poison? The sulfur-induced promotion of the bonding of unsaturated hydrocarbons on Cu(111). *J. Phys. Chem. B* **2006,** *110*, 21857-21864.

(90) Merino-Diez, N.; Lobo-Checa, J.; Nita, P.; Garcia-Lekue, A.; Basagni, A.; Vasseur, G.; Tiso, F.; Sedona, F.; Das, P. K.; Fujii, J.; et al. Switching from Reactant to Substrate Engineering in the Selective Synthesis of Graphene Nanoribbons. *J. Phys. Chem. Lett.* **2018,** *9*, 2510-2517.

(91) Ji, P. H.; MacLean, O.; Galeotti, G.; Dettmann, D.; Berti, G.; Sun, K. W.; Zhang, H. M.; Rosei, F.; Chi, L. F. Oxygen-promoted synthesis of armchair graphene nanoribbons on Cu(111). *Science China-Chemistry* **2021,** *64*, 636-641.

(92) Sanchez-Sanchez, C.; Martinez, J. I.; del Arbol, N. R.; Ruffieux, P.; Fasel, R.; Lopez, M. F.; de Andres, P. L.; Martin-Gago, J. A. On-Surface Hydrogen-Induced Covalent Coupling of Polycyclic Aromatic Hydrocarbons via a Superhydrogenated Intermediate. *J. Am. Chem. Soc.* **2019,** *141*, 3550-3557.

(93) Liu, M. Z.; Liu, M. X.; She, L. M.; Zha, Z. Q.; Pan, J. L.; Li, S. C.; Li, T.; He, Y. Y.; Cai, Z. Y.; Wang, J. B.; et al. Graphene-Like Nanoribbons Periodically Embedded with Four- and Eight-Membered Rings. *Nat. Commun.* **2017,** *8*, 14924.

(94) Feng, K.; Solel, E.; Schreiner, P. R.; Fuchs, H.; Gao, H. Y. Diamantanethiols on Metal Surfaces: Spatial Configurations, Bond Dissociations, and Polymerization. *J. Phys. Chem. Lett.* **2021,** *12*, 3468-3475.
(95) Kawai, S.; Krejci, O.; Nishiuchi, T.; Sahara, K.; Kodama, T.; Pawlak, R.; Meyer, E.; Kubo, T.; Foster, A. S. Three-dimensional graphene nanoribbons as a framework for molecular assembly and local probe chemistry. *Sci. Adv.* **2020,** *6*, eaay8913.
(96) Sosa-Vargas, L.; Kim, E.; Attias, A. J. Beyond "decorative" 2D supramolecular self-assembly: strategies towards functional surfaces for nanotechnology. *Materials Horizons* **2017,** *4*, 570-583.
(97) Bartels, L.; Meyer, G.; Rieder, K. H. Controlled vertical manipulation of single CO molecules with the scanning tunneling microscope: A route to chemical contrast. *Appl. Phys. Lett.* **1997,** *71*, 213-215.
(98) Horcas, I.; Fernández, R.; Gómez-Rodríguez, J. M.; Colchero, J.; Gómez-Herrero, J.; Baro, A. M. WSXM: A software for scanning probe microscopy and a tool for nanotechnology. *Rev. Sci. Inst.* **2007,** *78*, 013705.
(99) Necas, D.; Klapetek, P. Gwyddion: an open-source software for SPM data analysis. *Cent. Eur. J. Phys.* **2012,** *10*, 181-188.
(100) Kresse, G.; Hafner, J. Ab initio molecular dynamics for liquid metals. *Phys. Rev. B* **1993,** *47*, 558-561.
(101) Kresse, G.; Furthmuller, J. Efficient iterative schemes for ab initio total-energy calculations using a plane-wave basis set. *Phys. Rev. B* **1996,** *54*, 11169-11186.
(102) Perdew, J. P.; Ernzerhof, M.; Burke, K. Rationale for mixing exact exchange with density functional approximations. *J. Chem. Phys.* **1996,** *105*, 9982-9985.
(103) Blöchl, P. E. Projector augmented-wave method. *Phys. Rev. B* **1994,** *50*, 17953-17979.
(104) Kresse, G.; Joubert, D. From ultrasoft pseudopotentials to the projector augmented-wave method. *Phys. Rev. B* **1999,** *59*, 1758-1775.
(105) Grimme, S.; Antony, J.; Ehrlich, S.; Krieg, H. A consistent and accurate ab initio parametrization of density functional dispersion correction (DFT-D) for the 94 elements H-Pu. *J. Chem. Phys.* **2010,** *132*, 154104.
(106) Humphrey, W.; Dalke, A.; Schulten, K. VMD: Visual molecular dynamics. *Journal of Molecular Graphics & Modelling* **1996,** *14*, 33-38.
(107) Hapala, P.; Kichin, G.; Wagner, C.; Tautz, F. S.; Temirov, R.; Jelinek, P. Mechanism of high-resolution STM/AFM imaging with functionalized tips. *Phys. Rev. B* **2014,** *90*, 085421.
(108) Hapala, P.; Temirov, R.; Tautz, F. S.; Jelinek, P. Origin of High-Resolution IETS-STM Images of Organic Molecules with Functionalized Tips. *Phys. Rev. Lett.* **2014,** *113*, 226101.

TOC Graphics